Journal of Visualization, Vol. 3, No. 3 (2000) 275-285

Visualization of Multiple Scalar and Velocity Fields in a Lifted Jet Flame

Watson, K. A.*1, Lyons, K. M.*1, Donbar, J. M.*2 and Carter, C. D.*3

*1 Department of Mechanical and Aerospace Engineering, North Carolina State University, Box 7910, Raleigh, NC 27695-7910, USA.
*2 Air Force Research Laboratory, Wright-Patterson Air Force Base, OH 45433-7103, USA.
*3 Innovative Scientific Solutions, Inc., 2786 Indian Ripple Road, Dayton, OH 45440-3696, USA.

Received 21 July 1999.
Revised 22 November 1999.

***Abstract*:** The stabilization of lifted jet diffusion flames has long been a topic of interest to combustion researchers. The flame and flow morphology, the role of partial premixing, and the effects of large scale structures on the flame can be visualized through advanced optical imaging techniques. Many of the current explanations for flame stabilization can benefit from the flow and flame information provided by laser diagnostics. Additionally, the images acquired from laser diagnostic experiments reveal features invisible to the eye and line-of-sight techniques, thereby allowing a deeper insight into flame stabilization. This paper reports visualizations of flame and flow structures from Particle Image Velocimetry (PIV), Planar Laser-Induced Fluorescence (PLIF) and Rayleigh scattering. The techniques are surveyed and the success of visualization techniques in clarifying and furthering the understanding of lifted-jet flame stabilization is discussed.

***Keywords*:** laser diagnostics, combustion, jet diffusion flame, flame stabilization, particle image velocimetry (PIV), laser-induced fluorescence (LIF), Rayleigh scattering.

1. Introduction

Experimental fluid mechanics and combustion research have included a wide variety of techniques to study both large-scale and small-scale features of reacting and non-reacting flows. A non-intrusive category of techniques that has seen extensive use in these areas is that of laser diagnostics, where highly sensitive experimental methods have been developed to measure quantities by optical means. These techniques utilize various properties of the laser source which make it especially desirable for applications involving combustion. Lasers are spectrally narrow and many are tunable, making them ideal for probing specific molecules and radicals in reacting flows. The intense, collimated laser beam allows for focusing of the light into small resolution volumes in the form of light sheets, producing images with high signal levels, low noise and excellent spatial resolution. Many lasers can be pulsed, allowing energy to be delivered in a short time duration which, in effect, freezes the flow at that instant. Furthermore, laser diagnostics can often be applied in environments too hostile for even the most robust physical probes.

Some of the drawbacks in using lasers as probes include the need for optical access, the cost, and the relative level of skill necessary to perform these types of measurements. Among the most commonly employed techniques are elastic scattering from particles (Lorenz-Mie scattering) and molecules (Rayleigh scattering), planar laser-induced fluorescence (PLIF), Raman scattering and a host of nonlinear optical techniques. Eckbreth (1996) surveys the fundamental physics of the laser diagnostic techniques and describes their application in combustion phenomena. Another recent volume edited by Taylor (1993) surveys some of the more important instrumentation

and experimental approaches used in combustion diagnostics. Adrian (1991) and Laurenco et al. (1989) discuss velocity field measurement techniques, particularly particle image velocimetry (PIV).

From a fluid mechanics and combustion perspective, large-scale structures are believed to play an important role in the evolution of the flow and the structure of the flamefront. Traditionally, efforts have been made to characterize these systems by examining the statistics of a series of point measurements. Approaches of this kind have made great strides in gaining insight into these systems statistically, but often lack insight into important length scales and the formation and pathways of structural features. For this reason there is motivation to not only visualize the flowfield, as in some refractive techniques, but instantaneously measure the distribution of important scalar and vector quantities. Measurements of two-dimensional scalar fields provide a means of evaluating instantaneous spatial gradients of the scalar, which is not possible with point measurements. Measurements of two-dimensional velocity fields allow for the acquisition of instantaneous strain rates and provide limited information on vorticity. Furthermore, quantitative "pictures" often reveal essential features of flows and flames which cannot be revealed by point measurements.

In this paper, the role of visualization techniques in understanding lifted diffusion flame stabilization is discussed. An understanding of the stability of turbulent diffusion flames is important because of their widespread appearance in combustion applications. At lower jet velocities, diffusion flames often appear laminar near the jet exit and turbulent further downstream. As the flow velocity is increased, the flame becomes turbulent throughout before combustion ceases at the nozzle exit, resulting in a turbulent flame that is detached from the nozzle and stabilized in an axial ring a certain distance above the nozzle exit. The lifted jet flame (Fig. 1) is a system which allows an investigation of the flow/flame interactions that stabilize the flamefront and locally extinguish the combustion process further downstream. This information is important in understanding flame stability in industrial oil furnaces and burners, gas turbines and oil well fires, in addition to their methods of extinction. Flow visualization and laser diagnostic measurements are extremely useful in investigating issues such as the nature of the flame and the flow/flame interaction near the stabilization region. The extent of premixing at the flame front and its role as a stabilization mechanism is a common source of disagreement among current theories. Pitts (1988, 1989) discusses the major theories that have been developed. Earlier treatment of the problem centered around the belief that the base of the lifted flame lies in a stoichiometric premixed turbulent region. In a frequently referenced study, Vanquickenborne and Van Tiggelen (1966) propose that the stabilization of the flame results from equilibrium between the premixed turbulent burning velocity and the mean axial flow velocity. Other studies dismiss this explanation, arguing that the extinction of laminar diffusion flamelets is responsible for lifted flame stabilization (Peters and Williams, 1983). More recently, triple, or tribrachial, flames have received substantial consideration as the anchoring mechanism for lifted flames (Muñiz and Mungal, 1997; Schefer and Goix, 1998). Triple flames consist of an ordinary diffusion flame surrounded by two premixed flames, one fuel-rich and one fuel-lean, which join at the triple point. The two premixed zones allow for flame propagation against the incoming unburned flow while the trailing diffusion flame extends downstream from the premixed regions. With these previous studies in mind, the objectives of this paper are to report visualizations of the stabilization region of a lifted flame, review approaches to field measurements in lifted flames, and discuss the use of multiple parameter fields in assessing flame stabilization theories.

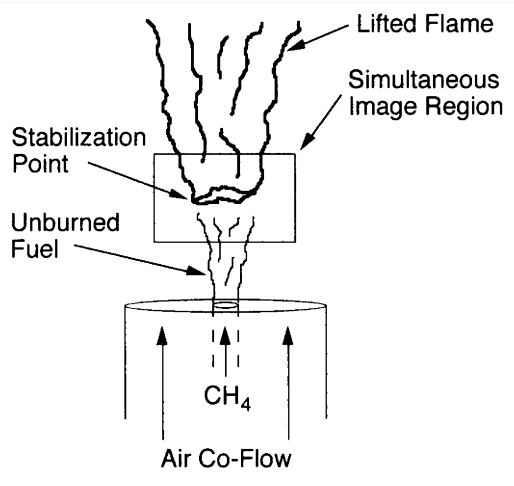

Fig. 1. Measurement location for the lifted flame experiments of this investigation.

2. Experimental Issues

Visualizations from three distinct experimental efforts are presented, each involving CH-PLIF measurements in conjunction with another laser diagnostic approach. The first experiment is a simultaneous measurement of the 2-D velocity field by particle image velocimetry and a visualization of the flamefront by CH fluorescence. This experiment is conducted to measure the velocity in the vicinity of the reaction zone indicated by the CH radical, which marks the fuel-rich side of the reaction zone. The second class of images report simultaneous visualizations of the flamefront by CH and OH fluorescence. The joint CH/OH measurements reveal visualizations of the fuel-rich (CH) and product (OH) sides of the reaction zone. The third class of measurements locates the reaction zone by CH fluorescence while visualizing the fuel/air mixing and high temperature regions of the flowfield by elastic Rayleigh scattering. Details of the various experimental techniques are briefly described; more complete discussions are presented by Carter et al. (1998) and Watson et al. (1999a and to appear).

A schematic representation of the experimental setup for the simultaneous PIV/CH-PLIF measurements is shown in Fig. 2. The co-flow burner consists of a 5-mm inner diameter fuel jet surrounded by a concentric 150-mm co-flow annulus. Methane was delivered through the fuel jet while low-speed air passed through the co-flow tube, resulting in the lifted flame sketched in Fig. 1. The laser sheets were oriented to illuminate an axial slice through the centerline of the flow and the two detectors were aligned such that the same region of the flow was imaged by the simultaneous measurements.

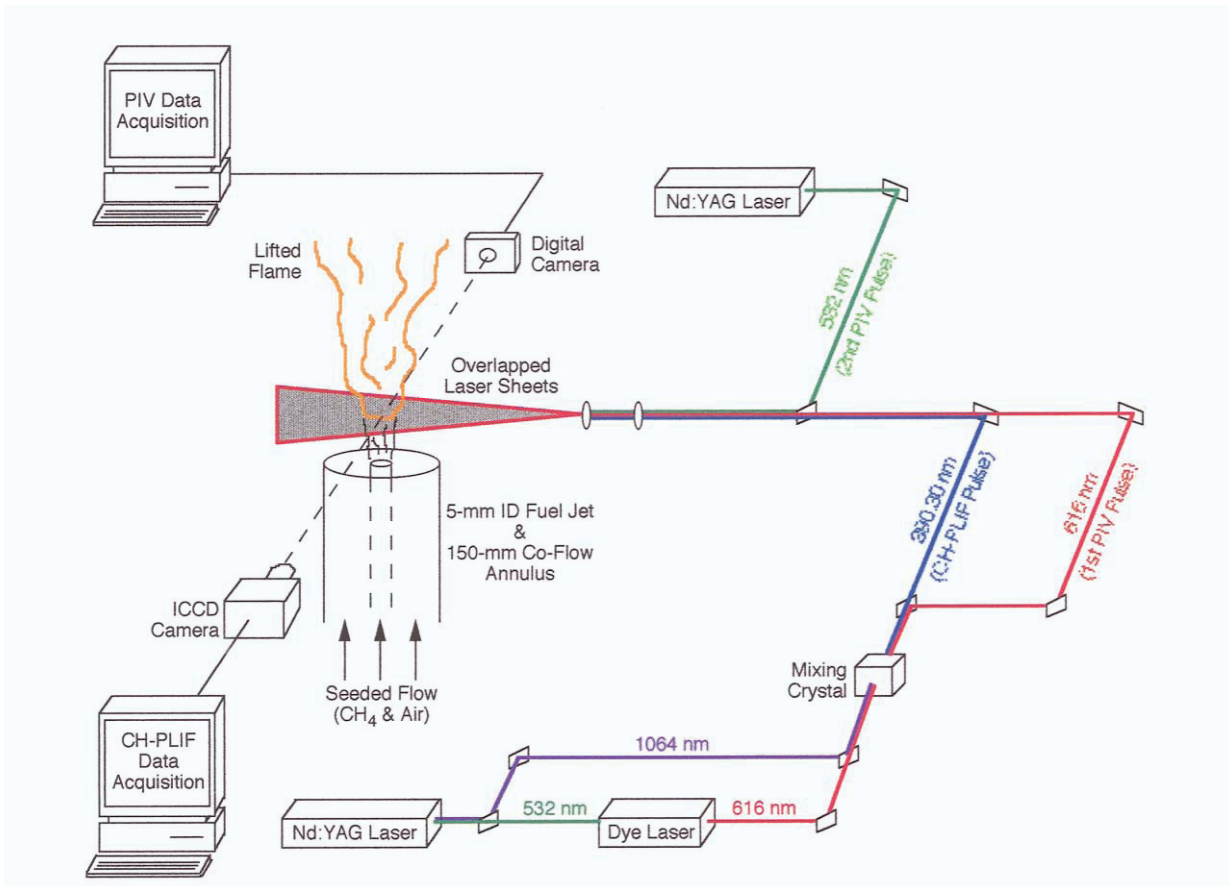

Fig. 2. Simultaneous PIV/CH-PLIF experimental arrangement.

For the PIV measurements, both the air and the methane streams were seeded with 0.5 μm alumina (Al_2O_3) particles. A two-color (red-green) PIV system was used which eliminates any directional ambiguity (Goss et al., 1991). The 616 nm (red) first PIV pulse was produced by a frequency-doubled Nd:YAG laser pumping a dye laser. The 532 nm (green) second PIV pulse was generated by a separate frequency-doubled Nd:YAG laser. Each pulse was expanded into a sheet before overlapping and illuminating the seed particles within the lifted methane flame. The time separation (Δt) between the two pulses was 60 μs. The PIV images were recorded with a

shuttered (5 ms) 3000 2000 pixel Kodak DCS-460 digital camera equipped with a 105-mm Nikkor lens operating at f#5.6. The images represent a 35.9 mm (radial direction) 23.9 mm (axial direction) region of the flow near the stabilization point of the lifted flame. The data was processed using customized two-color cross-correlation PIV software developed by Innovative Scientific Solutions, Inc. (ISSI). The vectors presented in this study result from 64 64 pixel interrogation regions with 50% overlap; each vector represents the average velocity from a 0.75-mm-square interrogation region.

The setup for the CH imaging technique includes a Nd:YAG-pumped dye laser which excites the $Q_1(7.5)$ transition of the $B^2\Sigma^- X^2\Pi(0,0)$ band of CH (λ = 390.30 nm). Fluorescence from the A-$X(1,1)$, (0,0) and B-$X(0,1)$ bands between λ = 420 and 440 nm was recorded. The 390 nm laser pulse was formed by mixing the 1064 nm output of the Nd:YAG laser with the 616 nm output of the dye laser within a mixing crystal. The fluorescence image was detected by a 576 384 pixel Princeton Instruments intensified CCD camera equipped with a 58-mm/f#1.2 Noct-Nikkor lens. Schott KV-418 and BG-1 color glass filters assured the CH fluorescence between 420 and 440 nm was transmitted while additional scattering from the 390 and 616 nm laser sources were rejected. The rectangular CH-PLIF images represent the same 35.9-mm-high 23.9-mm-wide region of the flow examined by the PIV images. Furthermore, the relative intensity of the CH-PLIF signal is not evident in the scalar images presented in this study and they should only be viewed as a qualitative indication of CH radical location.

The experimental configuration for the simultaneous CH/OH-PLIF experiment is not shown; however most of the arrangement is similar to the PIV/CH-PLIF schematic shown in Fig. 2. The differences are that the seed particles used for the PIV measurements are no longer present in the fuel and air streams, the first PIV pulse (616 nm) no longer enters the test section, and the portions of the experiment used for the second (532 nm) PIV pulse and the PIV detection are replaced by the OH imaging system. The OH-PLIF technique involves exciting the $R_1(8.5)$ transition of the $A^2\Sigma^+ X^2\Pi(1,0)$ band of OH with a laser source tuned to 281.3 nm. This sheet was produced by frequency-doubling the 562.6 nm output of a dye laser that is pumped by the second harmonic of a Nd:YAG laser. Fluorescence from the (1,1) and (0,0) bands was detected near 310 nm. The OH images were gathered by a second 576 384 pixel Princeton Instruments ICCD camera equipped with a 105-mm lens operating at f#4.5. Schott WG-295 and UG-5 filters assured that only the OH fluorescence near 310 nm was detected. Again, the OH-PLIF images correspond to the same 35.9 mm 23.9 mm region of flow examined by the CH-PLIF images.

The simultaneous Rayleigh scattering/CH-PLIF experimental arrangement is also similar to Fig. 2. The major difference is in the Rayleigh signal acquisition (once again, the 616 nm first PIV pulse does not enter the test section and the flow is not seeded). The Rayleigh scattering was generated by the 532 nm output of a Nd:YAG laser and detected by a PixelVision back-illuminated CCD camera equipped with a 58-mm/f#1.2 Noct-Nikkor lens and a 10-nm bandpass (FWHM) interference filter centered at 532 nm. To minimize background luminosity from the flame, a liquid crystal shutter (shuttering time = 200 μs) was placed between the lens and the camera body while a hood extension was directly attached to the lens. The horizontal (radial) field-of-view of the Rayleigh images matches the CH-PLIF image region and the top of the simultaneous images coincide. However, the larger streamwise field-of-view in the square Rayleigh images includes more of the non-reacting flow below the stabilization point. Furthermore, all Rayleigh images were normalized with respect to response images obtained in air to account for the irradiance distribution across the laser sheet.

3. Results

3.1 PIV/CH-PLIF Results

The simultaneous PIV/CH-PLIF measurements provide a means of establishing the velocity at the stabilization point of a lifted flame. This velocity is important because it can be compared to the premixed burning velocity, which in conjunction with other measurements allows an assessment of the extent of premixing at the flame base. Figure 3 is a simultaneous PIV/CH-PLIF image near the stabilization point of a lifted methane flame (CH_4 jet exit velocity = 21.8 m/s; lift-off height = 42.3 mm). Of particular significance is the rapid decay in the velocity field from a relatively high value near the jet center to a much lower value at the stabilization point near the outer edge of the fuel jet (1.1 m/s). Watson et al. (1999a) report stabilization region flow velocities that are relatively low (1.18 m/s on average) and appear to be limited by $3S_L$, where S_L is the premixed laminar burning velocity (S_L = 0.43 m/s for CH_4). Similar results regarding the flow velocity entering the stabilization region are presented by Muñiz and Mungal (1997) and Hasselbrink et al. (1998). The significance of these findings is that the turbulent flames

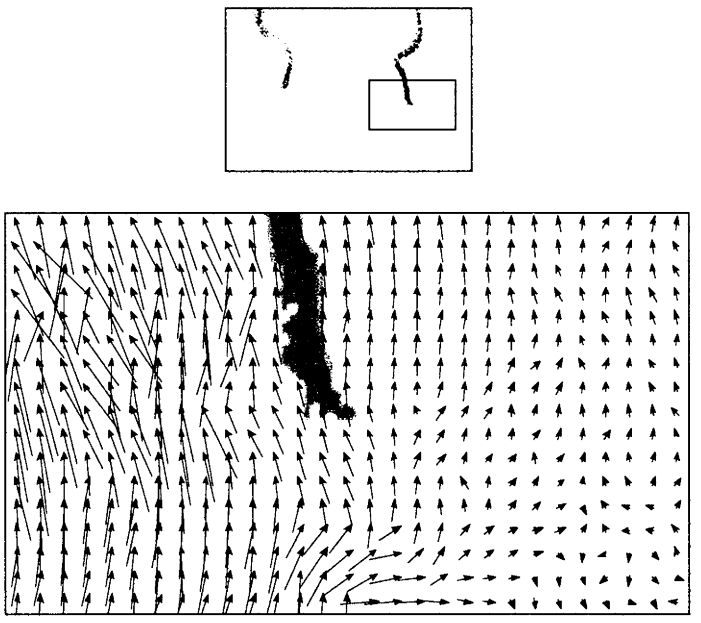

Fig. 3. Simultaneous PIV/CH-PLIF measurement from the boxed region of the top figure. Notice the relatively low velocity at the flame base where the magnitude is 1.1 m/s.

appear to be stabilized in a premixed, relatively low velocity region; the simultaneous Rayleigh scattering/CH-PLIF measurements discussed in Section 3.3 support this conclusion.

The relationship between the velocity field and the response of the flamefront as indicated by CH fluorescence was also explored by the simultaneous PIV/CH-PLIF experiment. While the stabilization region is very important, several observations can be made downstream of the flame base near regions of local flame extinction. Figure 4 is a visualization of the planar velocity field overlaid on the CH fluorescence image. The base of the lifted flame is just below the image region shown in the top figure and the bottom of that image is approximately 40 mm downstream from the jet exit (CH_4 jet exit velocity = 21.8 m/s). The opening in the CH radical field is believed to be a region where the combustion is locally extinguished and the corresponding velocity field highlights flow patterns that may have caused this occurrence. The formation of a internal vortex near the upper portion of the CH signal appears to be pushing the flame outward while flow enters the flame through the opening near the lower CH profile. This phenomenon of vortex-flame interactions leading to local flame extinction is consistent with previous findings by Takahashi et al. (1996) and Chen and Goss (1991). Internal vortices penetrating the reaction zone occur much more frequently than vortices generated within the surrounding air; the steep fuel concentration gradients ahead of these internally generated fuel vortices create excessive fuel fluxes into the reaction zone which quench exothermic reactions, reduce heat release, and cause local flame extinction as the vortex continues its radial motion into the flamefront.

As a visualization technique, this joint scalar/velocity approach reveals information about how the velocity field has an effect on the combustion zone. In regard to applying two-dimensional sheet imaging techniques to complex three-dimensional flows such as the turbulent lifted flames investigated in this study (Schefer, 1997), one cannot ignore possible out-of-plane motion. Nevertheless, the planar velocity measurements of this study, along with the scalar field observations discussed in the following sections, support the notion of vortex/flame interactions playing a crucial role in local flame extinction. Furthermore, these “holes” in the CH zone are not evident by eye nor discernible from line-of-sight techniques.

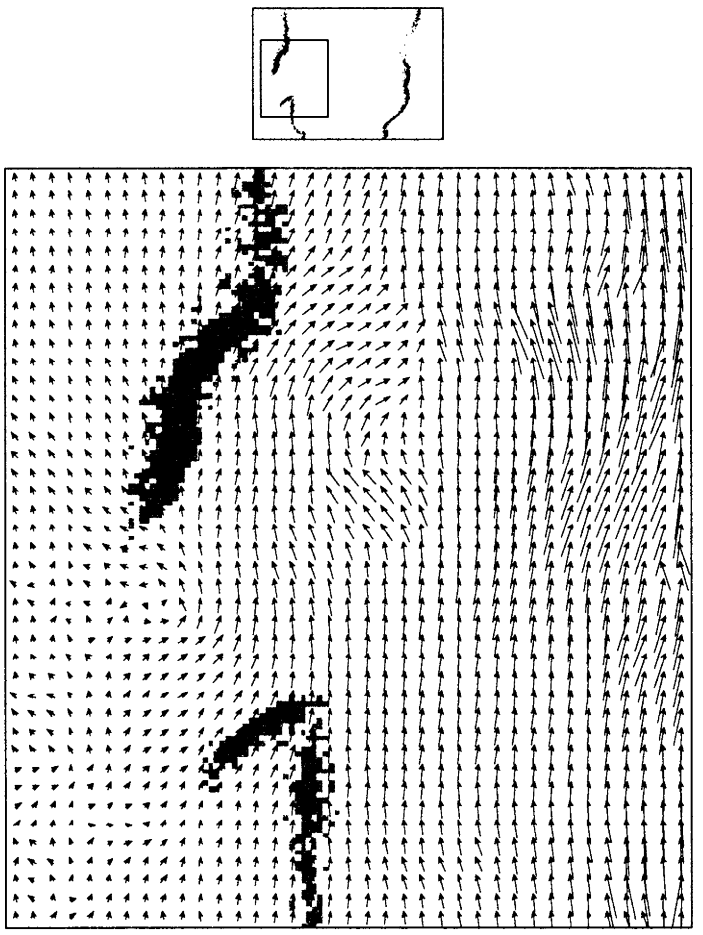

Fig. 4. Simultaneous PIV/CH-PLIF measurement from the boxed region of the top figure.

3.2 CH/OH-PLIF Results

Images of the CH zone provide information on fuel rich flame zone morphology and OH image data provide complementary information on the product side of the flame zone. With only one of these parameter fields, it is often difficult to discern the fuel side from the air side, particularly in more contorted flame structures. In addition, when "holes" are witnessed in both contours (Figs. 5(e)-(h)), one can conclude with great certainty that the combustion has locally ceased. A collection of joint CH/OH-PLIF images are shown in Fig. 5. The OH signal intensity is indicated in color, while the CH zone is represented by the thin black zone. The flow conditions are the same as the PIV/CH-PLIF experiment, while image locations vary depending upon the region examined. For example, the images in Figs. 5(a)-(d) are at a location which allows for an investigation of the fluctuating stabilization region, while the remaining images are shifted further downstream in an attempt to examine possible local extinction. Notice the CH profile is relatively thin (1.1 mm) and represents the fuel-rich side of the flame where fuel consumption is initiated, while the OH signal is much thicker (3.6 mm) and indicative of the fuel-lean portion where chemical reactions are completed. Several images in Fig. 5 complement the PIV/CH-PLIF findings. The right side of Figs. 5(a), (e) and the left side of Fig. 5(g) show bulges in both radical fields which support the vortex/flame interaction phenomenon discussed in the previous section. Furthermore, Figs. 5(e)-(h) show instances of local extinction where the lack of OH signal reinforces the openings in the CH profile. The left side of Fig. 5(g) is especially interesting where the bulge in both the CH and OH profile results in complete flame extinction as indicated by openings in both radical fields at the tip of this bulge. As the pocket of fuel that caused this bulge continues to radially penetrate the reaction zone, it is believed that the region of local extinction will widen. A sequential CH-PLIF/PIV experiment would be desirable to verify this progression and this will be performed in the future.

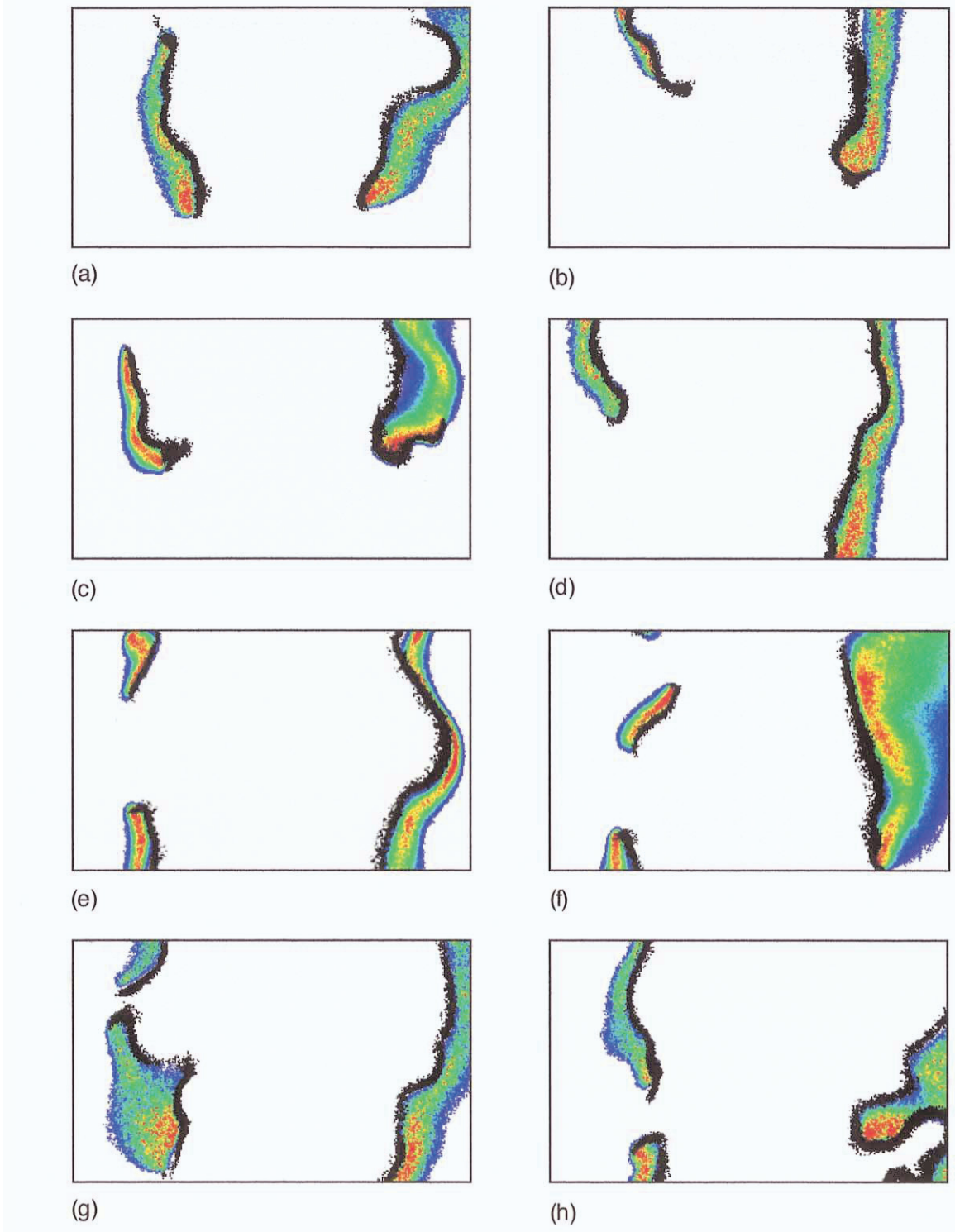

Fig. 5. Eight simultaneous CH/OH-PLIF measurements from a lifted flame. The OH intensity is indicated from low (purple) to high (red) and the CH region is represented by black.

A topic that is currently receiving considerable attention is the concept of a "leading edge" flame as the stabilization mechanism in lifted flames (Watson et al., 1999b). This leading edge refers to the outward-extending branch of CH at the base of the streamwise CH structure that may play a significant role in flame stabilization through partially premixed flame propagation. The radial curl in the CH zones witnessed on the right side of Figs. 5(b), (c) and the left side of Fig. 5(d) are possibly evidence of this feature. Watson et al. (1999b) contend that this observation, present in approximately 30% of images, provides evidence that partially premixed combustion plays a role in lifted flame stabilization. Researchers believe that these leading edge flames (see the right side of Figs.

5(b) and 5(c) may be a distorted triple flame. This "double flame" structure may result from quenching of one of the triple flame branches by the local flowfield and/or stoichiometry (Muñiz and Mungal, 1997; Wichman et al., 1997). Furthermore, the reason for its limited appearance may be due to the limitations of the 2-D imaging techniques. Specifically, the leading edge condition does not have to occur around the entire perimeter of the flame base and may be present at locations outside the image plane during instances where it is not seen. Whether the images presented here are examples of this circumstance is difficult to access; nevertheless, this topic demands consideration in future flame spread research.

In summary, the joint CH/OH-PLIF measurements show regions where combustion has ceased (i.e., lack of both CH and OH signals) and provide valuable information about the flamefront structure and morphology. This information may be useful in indicating which mechanism of flame stabilization is dominant at any given time.

3.3 Rayleigh Scattering/CH-PLIF Results

Figures 6 and 7 include simultaneous Rayleigh scattering (color) and CH-PLIF (white) measurements from two different flow conditions. The images in Fig. 6 correspond to the following flow conditions: CH_4 jet exit velocity = 21.2 m/s; air co-flow velocity = 0.13 m/s; *Re* = 6400. The bottom and top of the images are 25.4 and 61.3 mm from the jet exit, respectively. The Rayleigh images presented are only qualitative indications of the gas temperature with "hot" zones indicated by darker regions. Quantitative temperatures cannot easily be derived from

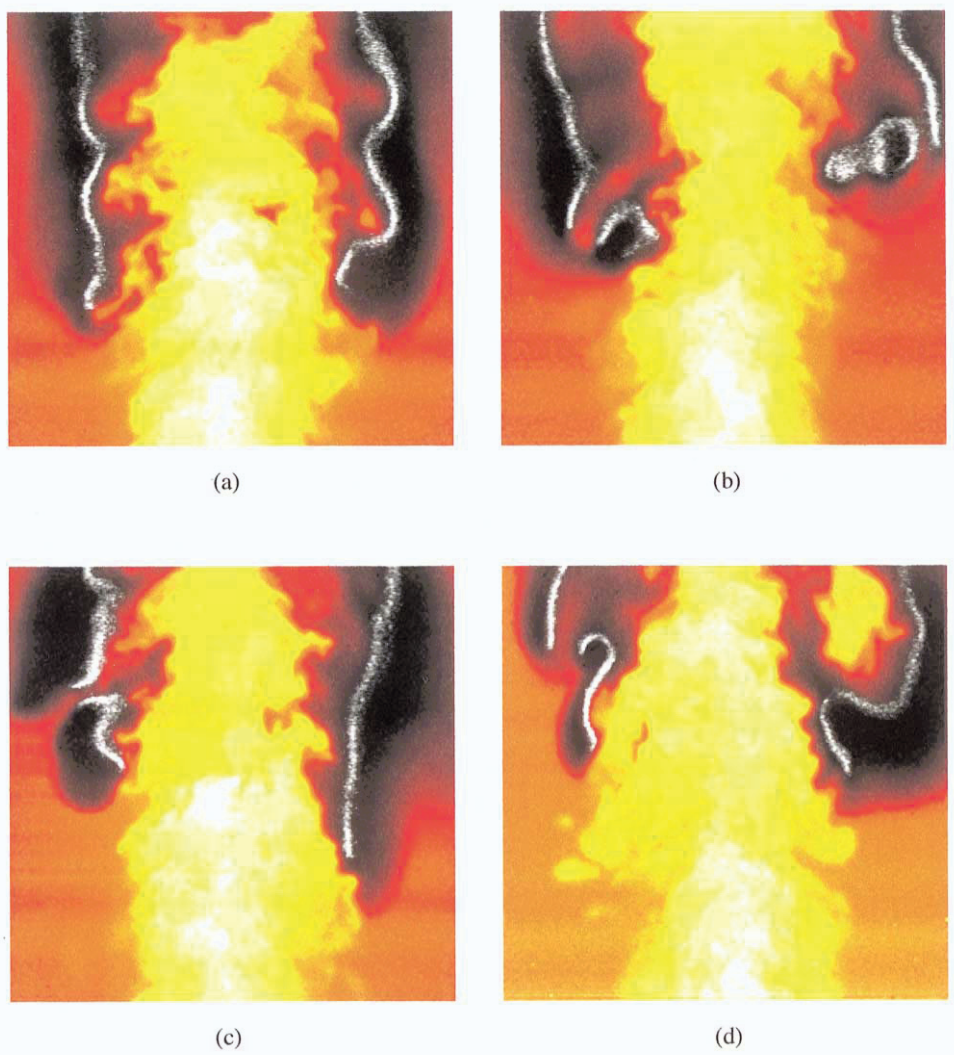

Fig. 6. Simultaneous Rayleigh scattering/CH-PLIF measurements from the *Re* = 6400 lifted flame. Rayleigh signal intensity is indicated from low (black) to high (white) while CH fluorescence is represented by the narrow white regions.

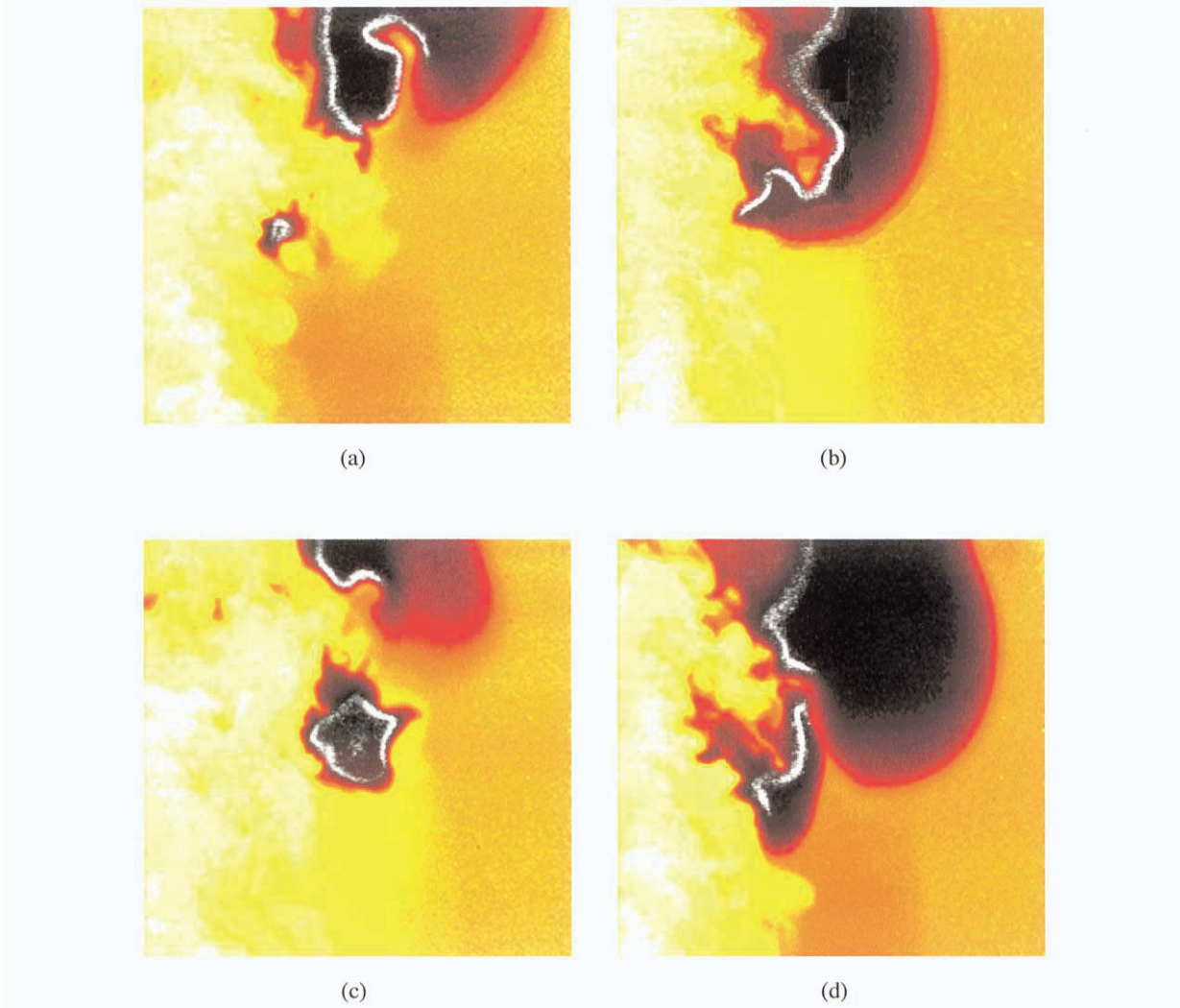

Fig. 7. Simultaneous Rayleigh scattering (color) and CH-PLIF (white) measurements from the *Re* = 8300 lifted flame. Only the right side of the flame is imaged due to the wider stabilization region resulting from higher flow conditions.

the Rayleigh signals in this experiment due to the difference in scattering cross-section between the methane and air ($\sigma_{fuel}/\sigma_{air} = 2.3$). Nonetheless, it is obvious that the Rayleigh images are excellent indicators of the flow behavior and provide information of the relative temperature in the reacting parts of the flame as well as the extent of premixing in isothermal regions below (i.e., upstream of) the combustion zone.

Several interesting features are highlighted by the Rayleigh images which definitively support the vortex/flame interactions described in the previous sections. Figure 6(a) includes bulges in the CH profile while the Rayleigh image indicates relatively colder fluid exists just inside the CH zone at these locations. This feature is evidence of the radial movement of large-scale fuel structures penetrating the reaction zone. A larger structure with even higher Rayleigh signal levels exists on the right side of Fig. 6(d) and the response of the CH profile to this fuel pocket is obvious. Figures 6(b)-(d) include breaks in the flamefront indicated by CH fluorescence which coincide with flow patterns indicated by the Rayleigh images. The left sides of these images show narrow streams of "colder" fluid connecting the inner-fuel jet to the surrounding air through openings in the CH zones. It would be difficult to assess the direction of the colder fluid passing through the reaction zone by examining the Rayleigh images alone; however, the CH profiles in Figs. 6(b)-(d) all include openings where the tips of the CH zones extend radially outward, providing convincing evidence that fluid originating from inside the lifted flame is responsible for the local extinction.

The images in Fig. 7 are from a higher flow condition (CH_4 jet exit velocity = 27.5 m/s; air co-flow velocity = 0.19 m/s; *Re* = 8400). The wider stabilization region that results from jet-spread at increased flow conditions limits these images to the right side of the lifted flame (i.e., the jet centerline is near the left side of the images in Fig. 7). The bottom and top of the images are 51.4 and 87.3 mm from the jet exit, respectively. Once again, several interesting flow patterns are visualized by the simultaneous measurements. A small portion of the CH zone has separated from the rest of the flame in Fig. 7(a) and the effects of this high temperature flame fragment are witnessed in the corresponding Rayleigh image. The two-dimensional nature of this technique renders it difficult to access whether this is in fact a flame fragment or actually the beginning of a larger reacting structure that extends out of the image plane. Figure 7(c) shows a much larger cellular structure that has separated from the rest of the lifted flame, while Fig. 7(b) suggests a colder "finger-like" projection originating from the fuel jet has penetrated the flame zone and caused a bulge in the CH profile. Finally, a small region of local extinction is evident in Fig. 7(d) where a narrow stream of relatively low temperature fluid connects the inner-fuel jet to the surrounding air.

The Rayleigh images also allow a determination of the extent of premixing of the fuel and air in the isothermal mixing region upstream of the stabilization zone. The Rayleigh images show that the state of the incoming reactants upstream of the stabilization region indicated by the CH zones are of a flammable mixture composition between the lean (5%) and rich (15%) flammability limits of methane in air (Everest et al., 1996; Watson et al., under review). As a result, the extent of premixing ahead of the CH zone and the relationship between the premixedness and the stabilization zone characteristics (i.e., CH zone structure, Rayleigh signal gradient, etc.) can be determined.

4. Conclusions and Discussion

This paper describes the role of visualization techniques in revealing important flowfield features involved in the stabilization of a lifted jet diffusion flame. The results from three sets of joint measurements (PIV/CH, CH/OH, CH/Rayleigh) have been presented and the rationale for each has been described. The effects of fuel vortices on the lifted flame have been shown and discussed. Complementary evidence for local extinction of the combustion process in lifted jet flames result from all three experiments. The importance of joint measurements is obvious; in these studies, the CH image locates the flame position while the other parameter field (velocity, OH fluorescence, Rayleigh scattering) allows for an evaluation of the flow behavior in the vicinity of the combustion zone. Without the CH image, the single parameter field is less relevant since its relationship to the location of the reaction zone remains unknown.

As technology progresses, researchers look forward to further developments in simultaneous laser diagnostic approaches. Currently, technical complications make the application of most of the techniques described in this paper difficult, if not impossible, to employ in a sequential fashion, in order to generate data sets that are close to real-time or near video rates. Furthermore, developments in three-dimensional techniques will be extremely beneficial to future research.

Acknowledgments

This work has been supported by National Science Foundation (Grants CTS-96-12740 and CTS-99-05786, Dr. Farley Fisher, Technical Monitor) and the Air Force Research Laboratory, Wright-Patterson Air Force Base, OH, under AFOSR Contract No. F33615-97-C-2702, Dr. Julian Tishkoff, Contract Monitor.

References

Adrian, R. J., Particle-imaging Techniques for Experimental Fluid Mechanics, Ann. Rev. Fluid Mech., 23 (1991), 261-304.

Carter, C. D., Donbar, J. M. and Driscoll, J. F., Simultaneous CH Planar Laser-Induced Fluorescence and Particle Imaging Velocimetry in Turbulent Nonpremixed Flames, Applied Physics B, 66 (1998), 129-132.

Chen, T. H. and Goss, L. P., Statistical OH-Zone Structures of Turbulent Jet Flames from Liftoff to Near-Blowout, Combustion Science and Technology, 79 (1991), 311-324.

Eckbreth, A., Laser Diagnostics for Combustion Temperature and Species, (1996), 2nd Edition, Gordon and Breach, The Netherlands.

Everest, D. A., Feikema, D. A. and Driscoll, J. F., Images of the Strained Flammable Layer Used to Study the Liftoff of Turbulent Jet Flames., Twenty-Sixth Symposium (International) on Combustion (1996), 129-136, The Combustion Institute, Pittsburgh.

Goss, L. P., Post, M. E., Trump, D. D. and Sarka, B., Two-Color Particle-Imaging Velocimetry, Journal of Laser Applications, (Winter 1991), 36-42.

Hasselbrink, E. F., Mungal, M. G. and Hanson, R. K., Simultaneous Planar Velocity Measurements and OH Imaging in a Transverse Jet Flame, Journal of Visualization, 1-1 (1998), 65-77.

Laurenco, L. M., Krothapalli, A. and Smith, C. A., Particle Image Velocimetry, in Advances in Fluid Mechanics Measurements, Lecture Notes in Engineering, (1989), Springer-Verlag, Heidelberg.

Muñiz, L. and Mungal, M. G., Instantaneous Flame-Stabilization Velocities in Lifted-Jet Diffusion Flames, Combustion and Flame, 111 (1997), 16-31.

Peters, N. and Williams, F. A., Liftoff Characteristics of Turbulent Jet Diffusion Flames, AIAA Journal, 21 (1983), 423-429.

Pitts, W. M., Assessment of Theories for the Behavior and Blowout of Lifted Turbulent Jet Diffusion Flames, Twenty-Second Symposium (International) on Combustion (1988), 809-816, The Combustion Institute, Pittsburgh.

Pitts, W. M., Importance of Isothermal Mixing Processes to the Understanding of Lift-Off and Blowout of Turbulent Jet Diffusion Flames, Combustion and Flame, 76 (1989), 197-212.

Schefer, R. W., Three-Dimensional Structure of Lifted, Turbulent-Jet Flames, Combustion Science and Technology, 125 (1997), 371-394.

Schefer, R. W. and Goix, P. J., Mechanism of Flame Stabilization in Turbulent, Lifted-Jet Flames, Combustion and Flame, 112 (1998), 559-574.

Takahashi, F., Schmoll, W. J., Trump, D. D. and Goss, L. P., Vortex-Flame Interactions and Extinction in Turbulent Jet Diffusion Flames, Twenty-Sixth Symposium (International) on Combustion (1996), 145-152, The Combustion Institute, Pittsburgh.

Taylor, A. M. K. P., Ed., Instrumentation for Flows with Combustion, (1993), Academic Press, San Diego.

Vanquickenborne, L. and Van Tiggelen, A., The Stabilization Mechanism of Lifted Diffusion Flames, Combustion and Flame, 10 (1966), 59-69.

Watson, K. A., Lyons, K. M., Donbar, J. M. and Carter, C. D., Scalar and Velocity Field Measurements in a Lifted CH_4-Air Diffusion Flame, Combustion and Flame, 117 (1999a), 257-271.

Watson, K. A., Lyons, K. M., Donbar, J. M. and Carter, C. D., Observations on the Leading Edge in Lifted Flame Stabilization, Combustion and Flame, 119 (1999b), 199-202.

Watson, K. A., Lyons, K. M., Donbar, J. M. and Carter, C. D., Simultaneous Rayleigh Imaging and CH-PLIF Measurements in a Lifted Jet Diffusion Flame, Combustion and Flame, (to appear).

Wichman, I. S., Lakkaraju, N. and Ramadan, B., The Structure of Quenched Triple Flames Near Cold Walls in Convective Flows, Combustion Science and Technology, 127 (1997), 141-165.

Author Profile

Kyle A. Watson: He received his M.S. from North Carolina State University in 1997 and is currently a Ph.D. candidate in Mechanical Engineering at the same university. His research interests are in flame stabilization and turbulent combustion.

Kevin M. Lyons: He received his Ph.D. in Mechanical Engineering from Yale University in 1994. His research interests are in the areas of flame stabilization, turbulent combustion and laser diagnostics. He is an Assistant Professor of Mechanical Engineering at North Carolina State University.

Jeffrey M. Donbar: He received his Ph.D. in Aerospace Engineering from the University of Michigan in 1998. Research interests include supersonic combustion, turbulent nonpremixed combustion, and laser diagnostics. He is currently a Research Scientist at the Air Force Research Laboratory, WPAFB, OH.

Campbell (Cam) D. Carter: He received his Ph.D. in Mechanical Engineering from Purdue University in 1990. His area of interest is laser diagnostics, particularly the application to reacting flows. He currently works for a small, employee-owned company, Innovative Scientific Solutions, Inc. (ISSI), involved in contract research.